$(SO_2CF_3)_2]$ was secured to the end of a glass fiber with 5-min epoxy resin. The crystal was maintained at −90 ± 1 °C during lineup and data collection. The crystal was found to belong to the monoclinic crystal class by the Enraf-Nonius CAD 4-SDP peak search, centering, and indexing programs.[40] Background counts were measured at both ends of the scan range with use of an ω–2θ scan, equal, at each side, to one fourth of the scan range of the peak. In this manner, the total duration of background measurements is equal to half of the time required for the peak scan. The intensities of three standard reflections were measured every 1.5 h of X-ray exposure, and no decay was noted. The data were corrected for Lorentz, polarization, and background effects and for the effects of absorption (μ = 22.0 cm^{-1}). An empirical absorption correction was applied by using the SDP program EAC.[39]

Solution and Refinement of the Structure. The structure was solved by conventional heavy-atom techniques. The Os atom was located by Patterson synthesis. Full-matrix least-squares refinement and difference-Fourier calculations were used to locate all the remaining hydrogen atoms. The atomic scattering factors were taken from the usual tabulation,[41] and the effects of anomalous dispersion were included in F_c by using Cromer and Ibers'[42] values of $\Delta f'$ and $\Delta f''$. In the final least-squares cycle, the largest parameter shift was 0.05 times its esd. The final difference-Fourier map did not reveal significant residual electron density except in the region approximately 1 Å from the Os atom. The highest peak in this region was 5 e Å^{-3}. Phenyl hydrogen atom positions were calculated (d_{C-H} set at 0.95 Å) and included in structure factor calculations but were not refined. The final positional and thermal parameters of the refined atoms appear in Table II and as supplementary material. The labeling scheme for the cation is presented in Figure S1. A table of observed and calculated structure factors is available as supplementary material.

The y coordinate of the Os atom is near $^1/_4$ so that the Os atoms are pseudo-B-centered. Since they dominate the scattering, this means that the entire structure appears to be pseudo-B-centered; that is, the $h + l$ odd reflections are all weak. The data set used, $F_o^2 \geq 2\sigma(F_o^2)$, gave an overall R = 0.095 with R = 0.084 for the $h + l$ even reflections and only R = 0.134 for the $h + l$ odd reflections only. Had we used the data set with $F_o^2 \geq 3\sigma(F_o^2)$, the overall R would have been 0.064, but this would have arisen by cutting out most of the $h + l$ odd reflections, which is inappropriate. The distances, angles, and least-squares planes within the phenyl rings (see supplementary material) are in good agreement with the expected values, which provides a good check on the quality of the structure.

Acknowledgment. We are grateful to members of the 3M Analytical and Properties Research Laboratory for the spectroscopic and analytical data and to Robert Koshar, 3M Industrial and Consumer Sector Research Laboratory, for gifts of fluorocarobn acids. L.H.P. also acknowledges support by the National Science Foundation of his contribution to this work.

Registry No. **6**, 88825-79-0; **6a**, 103530-21-8; **7**, 88825-81-4; **8**, 103439-64-1; **9**, 103439-75-4; **10**, 103439-66-3; **11**, 103439-68-5; **12**, 88841-59-2; $(Ph_3P)_3RuH_2(CO)$, 25360-32-1; $(Ph_3P)_3OsH_2(CO)$, 12104-84-6; $(Ph_3P)_3Ru(CO)Cl$, 103439-70-9; $(diphos)_2FeH_2$, 47898-23-7; $(Ph_3P)_3OsH_4$, 24228-59-9; $(diphos)_2FeHCl$, 32490-70-3.

Supplementary Material Available: Figure S1, an ORTEP view of the cation in **12** showing the labeling scheme, and tables of positional parameters and their estimated deviations, general temperature factor expressions, weighted least-squares planes, torsion angles, and distances and angles within phenyl rings in **12** (18 pages); a table of observed and calculated structure factor amplitudes (31 pages). Ordering information is given on any current masthead page.

---

[40] All calculations were carried out on PDP 8A and 11/34 computers with use of the Enraf-Nonius CAD 4-SDP programs. This crystallographic computing package is described: Frenz, B. A. In *Computing in Crystallography*; Shenk, H., Olthof-Hazekamp, R., van Konigsveld, H., Bassi, G. C., Eds.; Delft University Press: Delft, Holland, 1978; pp 64–71. *CAD 4 and SDP User's Manual*; Enraf-Nonius: Delft, Holland, 1978.

[41] Cromer, D. T.; Waber, J. T. *International Tables for X-Ray Crystallography*; Kynoch: Birmingham, England, 1974; Vol. IV, Table 2.2.4. Cromer, D. T. *Ibid.* Table 2.3.1.

[42] Cromer, D. T.; Ibers, J. A. In ref 38.

Contribution from the Department of Chemistry,
University of South Carolina, Columbia, South Carolina 29208

Ligand Substitution vs. Ligand Addition. 1. Differences in Reactivity between First- and Third-Row Transition-Metal Clusters. Reactions of Dimethylamine with the Sulfidometal Carbonyl Clusters $M_3(CO)_9(\mu_3\text{-}S)_2$ (M = Fe, Os)

Richard D. Adams* and James E. Babin

Received February 24, 1986

The reactions of the cluster complexes $M_3(CO)_9(\mu_3\text{-}S)_2$ (**1**, M = Fe; **3**, M = Os) with dimethylamine follow decidedly different pathways. The reaction with **1** yields the substitution product $Fe_3(CO)_8(Me_2NH)(\mu_3\text{-}S)_2$ (**2**) in 66% yield while the reaction with **3** yields the addition product $Os_3(CO)_8(\mu_3\text{-}S)_2(\mu\text{-}Me_2NC{=}O)(\mu\text{-}H)$ (**4**) in 93% yield. Both products have been characterized by IR and ^{1}H NMR spectroscopies and single-crystal X-ray diffraction analyses. For **2**, space group $P2_1/c$, a = 7.004 (1) Å, b = 13.652 (2) Å, c = 17.764 (2) Å, β = 91.87 (1)°, Z = 4, and ρ_{calcd} = 1.96 g/cm^3. The structure was solved by direct methods and was refined (1549 reflections) to the final values for the residuals R = 0.0437 and R_w = 0.0483. For **4**, space group $P2_1/c$, a = 9.223 (2) Å, b = 10.599 (4) Å, c = 19.773 (3) Å, β = 91.881 (16)°, Z = 4, and ρ_{calcd} = 3.20 g/cm^3. The structure was solved by direct methods and was refined (2485 reflections) to the final values of the residuals R = 0.0499 and R_w = 0.0583. The structure of **2** consists of an open triangular cluster of three iron atoms with two iron–iron bonds. There are triply bridging sulfido ligands on each side of the Fe_3 plane and a Me_2NH ligand positioned trans to one of the sulfido ligands on one of the external iron atoms. The structure of **4** consists of an open cluster having only one osmium–osmium bond, and it contains a bridging hydride ligand. There are two triply bridging sulfido ligands and a C,O-bonded bridging dimethylcarbamoyl ligand.

Introduction

Studies of the chemistry of transition-metal cluster compounds have revealed a variety of new and unusual ligand[1] and cluster[2] transformations. However, relatively few studies have been focused on the comparative reactivity of an homologous series of cluster compounds.[3] One of the good examples of such a study is that on the substitutional behavior of the tetranuclear clusters $M_4(CO)_{12}$ (M = Co, Rh, Ir) by phosphine and phosphite ligands.[3]

---

[1] Adams, R. D.; Horvath, I. T. *Prog. Inorg. Chem.* **1985**, *33*, 127.

[2] Vahrenkamp, H. *Adv. Organomet. Chem.* **1983**, *22*, 169.

[3] Muetterties, E. L.; Burch, R. R.; Stolzenberg, A. M. *Annu. Rev. Phys. Chem.* **1982**, *33*, 89 and references therein.

In this report we wish to describe the results of our investigations of the reactions of the sulfidometal carbonyl clusters $M_3(CO)_9(\mu_3\text{-}S)_2$ (M = Fe, Os) with dimethylamine. Recent studies of the reactions of primary and secondary amines with the clusters $M_3(CO)_{12}$ (M = Ru,[4] Os[5]) have revealed a pattern of amine addition to the carbonyl ligands that results in the formation of C,O-bonded bridging carbamoyl ligands.

Experimental Section

General Procedures. Although the reagents and products are air-stable, all reactions were performed under a dry-nitrogen atmosphere. Reagent grade solvents were dried over molecular sieves and were deoxygenated by purging with N_2 prior to use. Dimethylamine was obtained from Linde Corp. and was used without further purification. Infrared spectra were recorded on a Nicolet 5-DXB FT-IR spectrometer. A Brüker AM-300 FT-NMR spectrometer and an IBM NR-80 FT-NMR spectrometer were used to obtain ^1H NMR spectra. Elemental analyses were performed at MIC Anal., Tucson, AZ.

Preparation of $Fe_3(CO)_9(\mu_3\text{-}S)_2$ (1). A solution of $Fe_3(CO)_{12}$ (100 mg, 0.20 mmol) and ethylene sulfide (59 mL, 1.0 mmol) in hexane (100 mL) was refluxed under a slow purge of N_2 for 30 min. The solvent was removed in vacuo, and the residue was chromatographed on a Florisil column by eluting with *n*-hexane. A red band was collected and identified as **1** (52 mg (52%)) from its previously reported IR spectrum.[6]

Preparation of $Os_3(CO)_9(\mu_3\text{-}S)_2$ (3). In a similar manner, a solution of $Os_3(CO)_{12}$ (100 mg, 0.11 mmol) and ethylene sulfide (33 μL, 0.55 mmol) in 100 mL of octane solvent was refluxed for 3 h. After removal of the solvent in vacuo, the residue was chromatographed on a silica gel column by eluting with hexane. **3** (70 mg (70%)) was isolated and identified from its known IR spectrum.[7]

Reaction of 1 with Dimethylamine. At 25 °C a CH_2Cl_2 solution (100 mL) of **1** (50 mg, 0.10 mmol) was stirred for 90 min under an atmosphere of dimethylamine. The solvent was removed in vacuo, and the dark red product, $Fe_3(CO)_8(HNMe_2)(\mu_3\text{-}S)_2$ (**2**), was separated from unreacted **1** by TLC on silica gel plates by eluting with a 30% CH_2Cl_2/70% hexane solvent mixture. Yield: 17 mg, 66% (based on the amount of **1** consumed). IR $\nu(CO)$ in hexane solvent (cm^{-1}): 2076 (m), 2045 (w), 2033 (s), 2017 (vs), 2011 (s), 1995 (vw), 1967 (w), 1948 (vw). ^1H NMR in $CDCl_3$ solvent (δ): (at 80 MHz) 2.36 (d, 6 H, J_{H-H} = 6.1 Hz), 1.56 (br, 1 H); (at 300 MHz) 2.38 (t, 6 H, J_{H-H} = 5.6 Hz), 1.59 (br, 1 H). Anal. Calcd for **2**: C, 23.97; N, 2.79; H, 1.40. Found: C, 22.96; N, 2.79; H, 1.40.

Reaction of 3 with Dimethylamine. Dimethylamine was bubbled through a CH_2Cl_2 solution (40 mL) of **3** (30 mg, 0.034 mmol) at 25 °C until the bright yellow color had completely disappeared (approximately 2 min). After removal of the solvent in vacuo, the residue was dissolved in a minimum quantity of CH_2Cl_2 and this solution was chromatographed on silica TLC plates. Elution with a 25% CH_2Cl_2/75% hexane solvent mixture led to the isolation of $Os_3(CO)_8(\mu_3\text{-}S)_2(\mu\text{-}Me_2NC{=}O)(\mu\text{-}H)$ (**4**) (29.2 mg, (92.7%)). IR $\nu(CO)$ in hexane solvent (cm^{-1}): 2111 (m), 2091 (s), 2027 (vs), 2019 (s), 2001 (m), 1984 (vw), 1958 (m), 1516 (m, br). ^1H NMR (in $CDCl_3$, at 300 MHz) (δ): 3.64 (3 H), 3.13 (s, 3 H), −12.45 (s, 1 H). Anal. Calcd for **4**: C, 14.18; N, 1.50; H, 0.76. Found: C, 14.38; N, 1.46; H, 0.72.

Table I. Crystallographic Data for X-ray Diffraction Studies.

	2	**4**
	(A) Crystal Data	
formula	$Fe_3S_2O_8NC_{10}H_7$	$Os_3S_2O_9NC_{11}H_7$
space group	$P2_1/c$, No. 14	$P2_1/c$, No. 14
a, Å	7.004 (1)	9.223 (2)
b, Å	13.652 (2)	10.599 (4)
c, Å	17.764 (2)	19.774 (3)
β, deg	91.87 (1)	91.88 (2)
V, Å^3	1697.6	1931.9
M_r	500.8	931.8
Z	4	4
ρ_{calcd}, g cm^3	1.96	3.20
	(B) Measurement of Intensity Data	
radiation (λ, Å)	Mo Kα (0.71073)	Mo Kα (0.71073)
monochromator	graphite	graphite
detector aperture, mm		
horizn	2	2
vert	2	2
cryst faces	011, $0\bar{1}1$, $01\bar{1}$ $1\bar{1}\bar{4}$, $\bar{2}\bar{1}\bar{2}$, 212	$01\bar{1}$, $0\bar{1}1$, 100 $\bar{1}00$, 012, $0\bar{1}\bar{2}$
cryst size, mm	0.38 × 0.26 × 0.21	0.16 × 0.26 × 0.36
cryst orientation direction; deg from ϕ-axis	[100]; 1.2	[012]; 7.8
reflections measd	$+h,+k,\pm l$	$+h,+k,\pm l$
max 2θ, deg	48	50
ω-scan width, deg	1.1	1.1
scan type	moving cryst–stationary counter	moving cryst–stationary counter
bkgd (count time at each end of scan)	3.0	3.0
ω-scan rate,[a] deg/min	4	4
no. of reflcns measd	2872	4758
no. of data used ($F^2 \geq 3.0\sigma(F^2)$)	1549	2485
	(C) Treatment of Data	
abs cor	applied	applied
abs coeff, cm^{-1}	28.6	211.0
grid	14 × 8 × 8	10 × 10 × 10
transmissn coeff		
max	0.707	0.1209
min	0.590	0.0108
P factor	0.03	0.03
final residuals		
R_F	0.0437	0.0498
R_{wF}	0.0482	0.0583
esd of unit wt observn	1.58	2.041
largest shift/error value of final cycle	0.0	0.2
largest peak in final diff Fourier (e/Å^3)	0.6	2.5
no. of var	217	235

[a] Rigaku software uses a multiple–scan technique. If the $I/\sigma(I)$ ratio is less than 10.0, a second scan is made and the results are added to first scan, etc. A maximum of three scans was permitted per reflection.

Crystallographic Analyses. Dark red crystals of **2** and colorless crystals of **4** suitable for X-ray diffraction measurements were each grown by slow evaporation of solvent from solutions in a CH_2Cl_2/C_6H_{14} solvent mixture at −20 °C. Crystals were mounted in thin-walled glass capillaries. Diffraction measurements were made on a Rigaku AFC6 fully automated four-circle diffractometer by using graphite-monochromatized Mo Kα radiation. Unit cells were determined and refined from 25 randomly selected reflections obtained by using the diffractometer automatic search, center, index, and least-squares routines. Crystal data, data collection parameters, and results of the analyses are listed in Table I. All data processing was performed on a Digital Equipment Corp. MICROVAX I computer by using the TEXSAN structure solving program library obtained from Molecular Structure Corp., College Station, TX. Absorption corrections of a Gaussian integration type were done for both structures. Neutral-atom scattering factors were calculated by the standard procedures.[8a] Anomalous dispersion corrections were applied to all non-hydrogen atoms.[8b] Full-matrix least-squares refinements minimized the function

$$\sum_{hkl} w(|F_o| - |F_c|)^2$$

where $w = 1/\sigma(F)^2$, $\sigma(F) = \sigma(F_o^2)/2F_o$, and $\sigma(F_o^2) = [\sigma(I_{raw})^2 + (PF_o^2)^2]^{1/2}Lp$.

For both structures all non-hydrogen atoms were refined anisotropically. For **2** the N-bonded hydrogen atom of the dimethylamine ligand was located from a difference Fourier map, but for both structures the positions of the methyl hydrogen atoms were calculated by assuming idealized tetrahedral and staggered conformational geometries. The scattering contributions from the hydrogen atoms were added to the structure factor calculations, but their positions were not refined.

The unit cells and systematic absences for both compounds indicated that the crystals belonged to the monoclinic crystal system and the space

---

(4) Szostak, R.; Strouse, C. E.; Kaesz, H. D. *J. Organomet. Chem.* **1980**, *191*, 243.

(5) (a) Lin, Y. C.; Mayr, A.; Knobler, C. B.; Kaesz, H. D. *J. Organomet. Chem.* **1984**, *272*, 207. (b) Azam, K. A.; Yin, C. C.; Deeming, A. J. *J. Chem. Soc., Dalton Trans.* **1978**, 1201.

(6) Hiebler, W.; Gruber, J. A. *Z. Anorg. Allg. Chem.* **1958**, *296*, 91.

(7) Johnson, B. F. G.; Lewis, J.; Lodge, P. G.; Raithby, P. R.; Henrick, K.; McPartlin, M. *J. Chem. Soc., Chem. Commun.* **1979**, 719.

(8) *International Tables for X-ray Crystallography*; Kynoch: Birmingham, England, 1975; Vol. IV: (a) Table 2.2B, pp 99–101; (b) Table 2.3.1, pp 149–150.

Table II. Positional Parameters and B(eq) Values for $Fe_3(CO)_8(NHMe_2)(\mu_3\text{-}S)_2$ (**2**)

atom	x	y	z	B(eq), Å^2
Fe1	0.864 40 (17)	0.081 017 (85)	0.172 313 (64)	3.6
Fe2	0.831 66 (17)	0.268 071 (84)	0.161 956 (62)	3.0
Fe3	0.706 06 (16)	0.218 780 (80)	0.025 136 (61)	3.0
S2	0.982 00 (29)	0.172 74 (15)	0.079 26 (11)	3.3
S1	0.599 25 (30)	0.158 50 (15)	0.131 55 (11)	3.1
O12	1.242 9 (11)	0.048 78 (58)	0.244 75 (45)	8.0
O11	0.674 0 (10)	0.020 53 (52)	0.309 43 (37)	6.6
O13	0.825 4 (12)	−0.101 04 (54)	0.086 74 (39)	6.9
O22	1.184 8 (11)	0.291 26 (57)	0.253 18 (46)	5.5
O21	0.594 5 (11)	0.334 74 (54)	0.284 65 (41)	6.4
O23	0.858 6 (11)	0.456 90 (48)	0.084 56 (42)	7.3
O31	0.901 61 (95)	0.326 12 (55)	−0.092 34 (40)	7.9
O33	0.664 2 (10)	0.042 87 (50)	−0.064 90 (36)	5.3
N	0.439 04 (85)	0.281 98 (49)	0.002 14 (37)	3.5
C1	0.382 4 (14)	0.363 01 (72)	0.052 93 (57)	6.0
C2	0.396 1 (13)	0.310 80 (69)	−0.076 86 (54)	5.2
C12	1.096 9 (17)	0.061 04 (72)	0.214 74 (52)	5.9
C11	0.746 6 (13)	0.044 52 (61)	0.256 05 (50)	3.9
C13	0.840 8 (14)	−0.030 71 (72)	0.121 07 (50)	5.0
C22	1.048 7 (15)	0.280 09 (72)	0.217 64 (55)	4.3
C21	0.683 6 (14)	0.308 68 (67)	0.235 71 (53)	4.0
C23	0.839 1 (13)	0.381 32 (75)	0.110 41 (52)	4.6
C31	0.822 7 (12)	0.287 20 (63)	−0.046 25 (50)	4.1
C33	0.675 3 (12)	0.115 04 (72)	−0.031 79 (47)	3.6
H1	0.361 1	0.232 2	0.019 5	4.0
H11	0.381 7	0.339 4	0.096 1	4.0
H12	0.467 3	0.408 7	0.038 5	4.0
H13	0.239 3	0.398 2	0.044 4	4.0
H21	0.442 6	0.264 6	−0.113 3	4.0
H22	0.458 7	0.366 1	−0.073 5	4.0
H23	0.251 4	0.353 7	−0.072 4	4.0

Table III. Interatomic Distances with Esd's for $Fe_3(CO)_8(NHMe_2)(\mu_3\text{-}S)_2$ (**2**)[a]

atom	atom	dist	atom	atom	dist
Fe1	C13	1.78 (1)	Fe3	N	2.088 (6)
Fe1	C12	1.79 (1)	Fe3	S1	2.214 (2)
Fe1	C11	1.80 (1)	Fe3	S2	2.221 (2)
Fe1	S1	2.237 (3)	O12	C12	1.15 (1)
Fe1	S2	2.251 (2)	O11	C11	1.14 (1)
Fe1	Fe2	2.570 (2)	O13	C13	1.14 (1)
Fe2	C21	1.79 (1)	O22	C22	1.14 (1)
Fe2	C22	1.79 (1)	O21	C21	1.14 (1)
Fe2	C23	1.80 (1)	O23	C23	1.14 (1)
Fe2	S2	2.250 (2)	O31	C31	1.13 (1)
Fe2	S1	2.263 (2)	O33	C33	1.15 (1)
Fe2	Fe3	2.645 (2)	N	C2	1.48 (1)
Fe3	C33	1.75 (1)	N	C1	1.49 (1)
Fe3	C31	1.793 (9)			

[a] Distances are in angstroms. Estimated standard deviations in the least significant figure are given in parentheses.

group $P2_1/c$. The coordinates of the metal atoms in both structures were obtained by direct methods (MULTAN). All remaining non-hydrogen atoms were subsequently obtained from difference Fourier syntheses. The results of the final refinements for each structure are listed in Table I. Error analyses were calculated by using the inverse matrix obtained on the final cycle of refinement for each structure.

Results

The reaction of $Fe_3(CO)_9(\mu_3\text{-}S)_2$ (**1**) with Me_2NH yielded the product $Fe_3(CO)_8(NHMe_2)(\mu_3\text{-}S)_2$ (**2**) in 66% yield, based on the amount of **1** consumed in the reaction. The molecular structure of **2** was established from a single-crystal X-ray diffraction analysis. The crystallographic positional parameters are listed in Table II. Interatomic distances and angles are listed in Tables III and IV, respectively. An ORTEP drawing of the molecular structure of **2** is shown in Figure 1. Compound **2** is a Me_2NH-substituted derivative of the parent compound **1**. The cluster consists of an open triangle of three iron atoms with triply bridging sulfido ligands on opposite sides of the Fe_3 plane. The two iron–iron bonds are significantly different (Fe(1)–Fe(3) = 2.570 (2) Å and Fe(2)–Fe(3) = 2.645 (2) Å) but are similar to those found in **1** (2.582 (9) and 2.609 (10) Å).[9] The long iron–iron bond includes the substituted iron atom Fe(3). A similar lengthening effect was observed in the PMe_2Ph-substituted derivative of **3**.[10] The dimethylamine ligand is positioned trans to the sulfido ligand S(2) on Fe(3) (Fe(3)–N = 2.088 (6) Å, S(2)–Fe(3)–N = 164.3 (2)°).

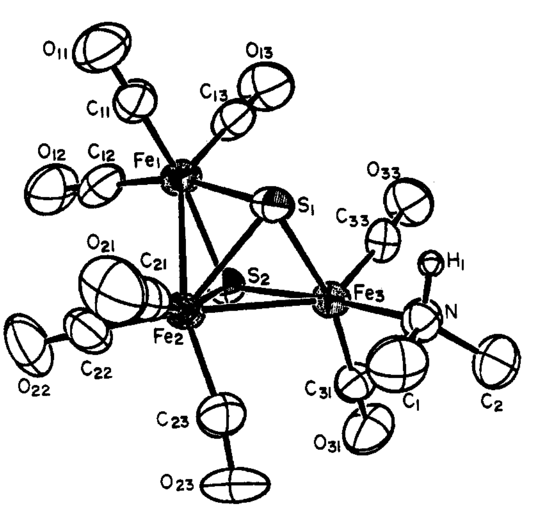

Figure 1. ORTEP diagram of $Fe_3(CO)_8(NHMe_2)(\mu_3\text{-}S)_2$ (**2**) showing 50% probability thermal ellipsoids. The hydrogen atom H(1) is shown with an artificially reduced thermal parameter, B = 1.0 Å^2.

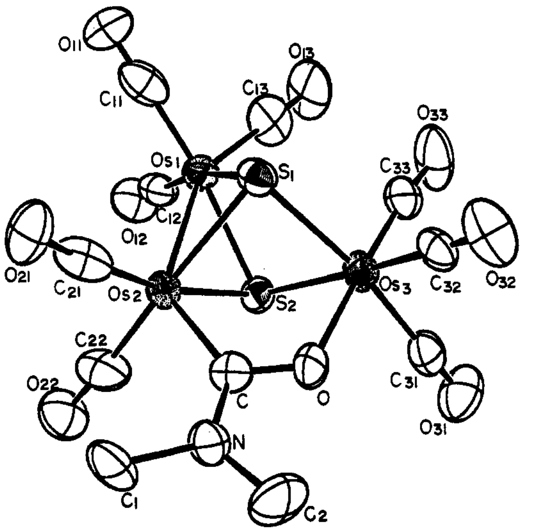

Figure 2. ORTEP diagram of $Os_3(CO)_8(\mu_3\text{-}S)_2(\mu\text{-}Me_2NC{=}O)(\mu\text{-}H)$ (**4**) showing 50% probability thermal ellipsoids.

The hydrogen atom, H(1), on the amine ligand was observed in a difference Fourier map in a chemically reasonable position (N–H(1) = 0.93 Å), but its location was not refined. Other molecular dimensions in **2** are similar to those in **1**.

At 80 MHz the ^1H NMR spectrum shows a doublet 2.36 ppm (J_{H-H} = 6.1 Hz) and a broad singlet at 1.56 ppm. The former can be assigned to the methyl resonances coupled to the NH proton. The latter must be the NH proton resonance, which is broadened by coupling to the nitrogen nucleus. At 300 MHz the ^1H NMR spectrum shows a triplet centered at 2.38 ppm (J_{H-H} = 5.6 Hz) and a broad singlet at 1.59 ppm. It appears that the triplet is a combination of two overlapping methyl doublets that are coupled to the NH proton resonance at 1.59 ppm. Inequivalence of the methyl groups is indicated by the structural analysis. Presumably, at 80 MHz the two resonances are accidently shift-equivalent.

---

(9) Wei, C. H.; Dahl, L. F. *Inorg. Chem.* **1965**, *4*, 493.

(10) Adams, R. D.; Horvath, I. T.; Segmuller, B. E.; Yang, L. W. *Organometallics* **1983**, *2*, 144.

Table IV. Interatomic Angles with Esd's for $Fe_3(CO)_8(NHMe_2)(\mu_3\text{-}S)_2$ (**2**)[a]

atom	atom	atom	angle	atom	atom	atom	angle	atom	atom	atom	angle
C13	Fe1	C12	98.8 (5)	C22	Fe2	S1	141.4 (3)	N	Fe3	S2	164.3 (2)
C13	Fe1	C11	98.5 (4)	C22	Fe2	Fe1	88.8 (3)	N	Fe3	Fe2	110.1 (2)
C13	Fe1	S1	100.2 (3)	C22	Fe2	Fe3	141.3 (3)	S1	Fe3	S2	80.72 (8)
C13	Fe1	S2	97.5 (3)	C23	Fe2	S2	98.2 (3)	S1	Fe3	Fe2	54.65 (6)
C13	Fe1	Fe2	143.9 (3)	C23	Fe2	S1	118.6 (3)	S2	Fe3	Fe2	54.24 (6)
C12	Fe1	C11	92.6 (4)	C23	Fe2	Fe1	152.5 (3)	Fe3	S2	Fe2	72.53 (8)
C12	Fe1	S1	160.2 (3)	C23	Fe2	Fe3	76.4 (3)	Fe3	S2	Fe1	98.12 (9)
C12	Fe1	S2	92.5 (3)	S2	Fe2	S1	79.05 (8)	Fe2	S2	Fe1	69.63 (7)
C12	Fe1	Fe2	105.0 (3)	S2	Fe2	Fe1	55.21 (6)	Fe3	S1	Fe1	98.7 (1)
C11	Fe1	S1	90.0 (3)	S2	Fe2	Fe3	53.23 (6)	Fe3	S1	Fe2	72.40 (7)
C11	Fe1	S2	162.2 (3)	S1	Fe2	Fe1	54.70 (7)	Fe1	S1	Fe2	69.65 (8)
C11	Fe1	Fe2	107.0 (3)	S1	Fe2	Fe3	52.95 (6)	C2	N	C1	109.1 (7)
S1	Fe1	S2	79.58 (8)	Fe1	Fe2	Fe3	80.75 (5)	C2	N	Fe3	116.7 (5)
S1	Fe1	Fe2	55.65 (6)	C33	Fe3	C31	93.6 (4)	C1	N	Fe3	116.3 (5)
S2	Fe1	Fe2	55.16 (6)	C33	Fe3	N	97.4 (3)	O12	C12	Fe1	177 (1)
C21	Fe2	C22	94.0 (4)	C33	Fe3	S1	98.9 (3)	O11	C11	Fe1	179.0 (8)
C21	Fe2	C23	97.7 (4)	C33	Fe3	S2	96.3 (3)	O13	C13	Fe1	178.4 (8)
C21	Fe2	S2	162.6 (3)	C33	Fe3	Fe2	140.2 (3)	O22	C22	Fe2	177 (1)
C21	Fe2	S1	87.1 (3)	C31	Fe3	N	94.1 (3)	O21	C21	Fe2	177.5 (9)
C21	Fe2	Fe1	108.0 (3)	C31	Fe3	S1	166.4 (3)	O23	C23	Fe2	172 (1)
C21	Fe2	Fe3	124.7 (3)	C31	Fe3	S2	92.5 (3)	O31	C31	Fe3	176.4 (8)
C22	Fe2	C23	99.4 (4)	C31	Fe3	Fe2	111.8 (3)	O33	C33	Fe3	174.4 (8)
C22	Fe2	S2	90.4 (3)	N	Fe3	S1	89.7 (2)				

[a] Angles are in degrees. Estimated standard deviations in the least significant figure are given in parentheses.

Table V. Positional Parameters and B(eq) Values for $Os_3(CO)_8(\mu_3\text{-}S)_2(\mu\text{-}Me_2NC{=}O)(\mu\text{-}H)$ (**4**)

atom	x	y	z	B(eq), Å^2
Os1	0.279597 (90)	0.147843 (91)	0.097508 (46)	3.3
Os2	0.003885 (79)	0.254270 (84)	0.076451 (41)	2.7
Os3	0.159743 (88)	0.394640 (87)	0.213894 (44)	2.8
S1	0.22875 (54)	0.37554 (54)	0.09623 (27)	3.1
S2	0.10165 (55)	0.17599 (53)	0.18542 (27)	3.0
O	−0.0526 (14)	0.4368 (14)	0.17956 (74)	3.1
O11	0.4404 (20)	0.1589 (21)	−0.0338 (10)	6.5
O12	0.2682 (19)	−0.1395 (18)	0.1010 (10)	5.7
O13	0.5636 (20)	0.1418 (23)	0.1813 (11)	7.0
O21	−0.0376 (19)	0.3599 (19)	−0.06505 (83)	5.5
O22	−0.2487 (18)	0.0723 (17)	0.06532 (97)	5.0
O31	0.0462 (21)	0.3767 (19)	0.35889 (94)	6.2
O32	0.2050 (19)	0.6817 (18)	0.21737 (96)	4.8
O33	0.4629 (19)	0.3449 (21)	0.2723 (11)	5.7
N	−0.2434 (17)	0.4393 (19)	0.11149 (85)	3.6
C	−0.1118 (20)	0.3914 (19)	0.12420 (98)	3.2
C1	−0.3313 (23)	0.4036 (28)	0.0499 (13)	4.7
C2	−0.2964 (26)	0.5421 (28)	0.1516 (14)	6.4
C11	0.3823 (25)	0.1532 (24)	0.0154 (16)	4.7
C12	0.2757 (22)	−0.0323 (28)	0.0998 (12)	4.3
C13	0.4552 (28)	0.1455 (24)	0.1493 (16)	5.5
C21	−0.0277 (22)	0.3205 (19)	−0.0108 (15)	4.2
C22	−0.1537 (25)	0.1470 (29)	0.0711 (13)	6.1
C31	0.0818 (24)	0.3896 (23)	0.3059 (13)	3.5
C32	0.1859 (21)	0.5748 (23)	0.2161 (11)	2.8
C33	0.3450 (25)	0.3648 (22)	0.2453 (13)	3.8

In a CH_2Cl_2 solution, $Os_3(CO)_9(\mu_3\text{-}S)_2$ (**3**) reacted rapidly (<2 min) with Me_2NH at 25 °C to give a 93% yield of the addition product $Os_3(CO)_8(\mu_2\text{-}Me_2NC{=}O)(\mu_3\text{-}S)_2(\mu\text{-}H)$ (**4**). The molecular structure of **4** was established from a single-crystal X-ray diffraction analysis. The crystallographic positional parameters are listed in Table V. Interatomic distances and angles are listed in Tables VI and VII, respectively. An ORTEP diagram of the molecular structure of **4** is shown in Figure 2. The molecule consists of an open cluster of three osmium atoms. Only one osmium–osmium separation is within the normal bonding range (Os(1)–Os(2) = 2.801 (1) Å), and this bond is believed to contain a bridging hydride ligand. The hydride ligand was not located crystallographically but was verified by its ^1H NMR signal (δ = −12.45 ppm). The Os(1)···Os(2) and Os(1)···Os(3) distances of 3.378 (1) and 3.678 (1) Å, respectively, are both much larger than the Os–Os bonding distance of 2.813 (1) Å found in **3** and indicate that little or no direct bonding exists between these atomic pairs.[10] Triply bridging sulfido ligands are symmetrically positioned about the Os_3 plane. All Os–S distances span the narrow range 2.440 (6)–2.460 (5) Å. These distances are slightly longer than those found in **1**, 2.390 (2)–2.454 (2) Å.[10] The most interesting ligand is a dimethylcarbamoyl ligand that bridges the atoms Os(2) and Os(3) via its carbon and oxygen atoms (Os(2)–C = 2.05 (2) Å and Os(3)–O = 2.10 (1) Å). The distances are slightly shorter than those of the corresponding bonds (2.121 (7) and 2.141 (4) Å) observed in the triosmium cluster $Os_3(CO)_9[PMe_2Ph](\mu\text{-}p\text{-}CH_3C_6H_4NHC{=}O)(\mu\text{-}H)$.[11] The C=O and C—N distances in **4** at 1.30 (2) and 1.33 (2) Å are similar to those found for carbamoyl ligands in other cluster complexes.[4,11,12] The short C–N distance implies the existence of partial multiple bonding between these atoms. Accordingly, the nitrogen atom has a planar geometry. The observation of two resonances for the inequivalent N-methyl groups indicates that rotation about the C–N bond is slow on the NMR time scale.

Table VI. Interatomic Distances with Esd's for $Os_3(CO)_8(\mu_3\text{-}S)_2(\mu\text{-}Me_2NC{=}O)(\mu\text{-}H)$ (**4**)[a]

atom	atom	dist	atom	atom	dist
Os1	C13	1.89 (3)	Os3	S2	2.440 (6)
Os1	C11	1.91 (3)	Os3	S1	2.441 (6)
Os1	C12	1.91 (3)	O	C	1.30 (2)
Os1	S2	2.448 (5)	O11	C11	1.13 (3)
Os1	S1	2.458 (6)	O12	C12	1.14 (3)
Os1	Os2	2.801 (1)	O13	C13	1.17 (3)
Os2	C22	1.85 (3)	O21	C21	1.15 (3)
Os2	C21	1.88 (3)	O22	C22	1.18 (3)
Os2	C	2.05 (2)	O31	C31	1.12 (3)
Os2	S2	2.453 (5)	O32	C32	1.15 (3)
Os2	S1	2.460 (5)	O33	C33	1.21 (3)
Os3	C33	1.83 (2)	N	C	1.33 (2)
Os3	C32	1.93 (2)	N	C2	1.44 (3)
Os3	C31	1.98 (3)	N	C1	1.49 (3)
Os3	O	2.10 (1)	Os1	Os3	3.678 (1)
			Os2	Os3	3.378 (1)

[a] Distances are in angstroms. Estimated standard deviations in the least significant figure are given in parentheses.

Discussion

The reactions of clusters **1** and **3** with dimethylamine produce vastly different results. The reaction of **1** results in a ligand

---

(11) Adams, R. D.; Golembeski, N. M.; Selegue, J. *Inorg. Chem.* **1981**, *20*, 1242.

(12) Boag, N. M.; Knobler, C. B.; Kaesz, H. D. *Angew. Chem., Int. Ed. Engl.* **1983**, *22*, 249.

Table VII. Interatomic Angles with Esd's for $Os_3(CO)_8(\mu_3\text{-}S)_2(\mu\text{-}Me_2NC{=}O)(\mu\text{-}H)$ (**4**)[a]

atom	atom	atom	angle	atom	atom	atom	angle	atom	atom	atom	angle
C13	Os1	C11	91 (1)	C21	Os2	S1	93.2 (6)	S2	Os3	S1	76.3 (2)
C13	Os1	C12	89 (1)	C21	Os2	Os1	113.6 (7)	Os3	S1	Os1	97.3 (2)
C13	Os1	S2	101.5 (9)	C	Os2	S2	91.0 (5)	Os3	S1	Os2	87.1 (2)
C13	Os1	S1	100.3 (8)	C	Os2	S1	90.3 (6)	Os1	S1	Os2	69.4 (2)
C13	Os1	Os2	147.6 (7)	C	Os2	Os1	134.4 (5)	Os3	S2	Os1	97.6 (2)
C11	Os1	C12	93 (1)	S2	Os2	S1	75.7 (2)	Os3	S2	Os2	87.3 (2)
C11	Os1	S2	164.6 (7)	S2	Os2	Os1	55.1 (1)	Os1	S2	Os2	69.7 (1)
C11	Os1	S1	93.6 (8)	S1	Os2	Os1	55.3 (1)	C	O	Os3	124 (1)
C11	Os1	Os2	109.6 (7)	C33	Os3	C32	93 (1)	C	N	C2	120 (2)
C12	Os1	S2	95.3 (7)	C33	Os3	C31	93 (1)	C	N	C1	122 (2)
C12	Os1	S1	167.9 (6)	C33	Os3	O	177.5 (8)	C2	N	C1	117 (2)
C12	Os1	Os2	112.9 (6)	C33	Os3	S2	96.3 (7)	O	C	N	112 (2)
S2	Os1	S1	75.9 (2)	C33	Os3	S1	92.3 (8)	O	C	Os2	116 (1)
S2	Os1	Os2	55.2 (1)	C32	Os3	C31	93 (1)	N	C	Os2	132 (2)
S1	Os1	Os2	55.3 (1)	C32	Os3	O	84.9 (7)	O11	C11	Os1	178 (2)
C22	Os2	C21	95 (1)	C32	Os3	S2	166.8 (6)	O12	C12	Os1	178 (2)
C22	Os2	C	92 (1)	C32	Os3	S1	93.9 (7)	O13	C13	Os1	179 (2)
C22	Os2	S2	96.2 (7)	C31	Os3	O	86.5 (7)	O21	C21	Os2	176 (2)
C22	Os2	S1	171.5 (8)	C31	Os3	S2	95.9 (7)	O22	C22	Os2	175 (3)
C22	Os2	Os1	118.0 (9)	C31	Os3	S1	171.2 (6)	O31	C31	Os3	173 (2)
C21	Os2	C	95.2 (9)	O	Os3	S2	86.1 (4)	O32	C32	Os3	178 (2)
C21	Os2	S2	167.3 (6)	O	Os3	S1	88.8 (4)	O33	C33	Os3	174 (2)

[a] Angles are in degrees. Estimated standard deviations in the least significant figure are given in parentheses.

substitution at one of the external iron atoms of the open cluster (route 1, M = Fe).

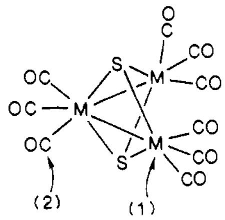

The reaction with **3** results in amine addition and formation of a C,O-bonded bridging *N*,*N*-dimethylcarbamoyl ligand. This occurs, presumably, by a direct attack of the amine at the carbon atom of one of the carbonyl ligands. It is well-known that primary and secondary amines will react with a variety of mononuclear metal carbonyl cluster compounds to yield products that contain carbamoyl ligands.[13] From the stereochemistry of the product, one would conclude that this addition occurred upon one of the carbonyl ligands attached to the central metal atom of the cluster (route 2, M = Os). The hydrogen atom on the amine is shifted to the metal atoms to become a hydride ligand. The oxygen atom of the carbamoyl ligand becomes bonded to a neighboring metal atom by donation of one of its lone pairs of electrons. This donation induces the cleavage of one of the two metal–metal bonds. Recent reports on the reactions of $Ru_3(CO)_{12}$ and $Os_3(CO)_{12}$ with primary and secondary amines described the products $M_3(CO)_{10}(\mu\text{-}R_2NC{=}O)(\mu\text{-}H)$ that also contained C,O-bonded bridging carbamoyl ligands. However, these reactions were accompanied by the loss of 1 mol of CO. As a result, the cleavage of a metal–metal bond was not observed.[4,5] There are very few examples of addition reactions to carbonyl ligands in cluster complexes that yield stable products in which a metal–metal bond has been cleaved. However, recent reports of the reactions of the carbido clusters $M_5(CO)_{15}(\mu_5\text{-}C)$ (M = Ru, Os) with methyllithium[14] and alcohols,[15] respectively, have described products consisting of open clusters containing bridging acetyl and bridging alkoxycarbonyl ligands.

An explanation for the greater ease of a substitution reaction of Me_2NH with **1** than with **3** could be due simply to the weaker metal–carbonyl bond strengths of **1** compared to those of **3**.[16] An explanation for the facility of amine addition to the CO ligands in **3** is less clear, but Angelici has shown that the formation of carbamoyl ligands by the addition of amine to CO ligands in mononuclear complexes is directly related to the CO bond strength (i.e., the greater the CO bond strength is, the greater the tendency to form carbamoyl ligands is). To a first approximation CO stretching frequencies are directly related to CO bond strength. All CO stretching frequencies for **3**[7] are higher than those of **1**.[6] Thus, according to Angelici's rule, **3** should exhibit a greater tendency to add amine at a CO group than **1** does. This is in accord with the results.

Acknowledgment. The research was supported by the National Science Foundation under Grant No. CHE-8416460. The AM-300 NMR spectrometer was purchased with funds from National Science Foundation Grant No. CHE-8411172. We wish to thank Johnson-Matthey, Inc., for a loan of osmium tetroxide.

Registry No. **1**, 22309-04-2; **2**, 103671-00-7; **3**, 72282-40-7; **4**, 103671-01-8; $Os_3(CO)_{12}$, 15696-40-9; $Fe_3(CO)_{12}$, 17685-52-8; $HNMe_2$, 124-40-3; CO, 630-08-0.

Supplementary Material Available: Tables of anisotropic thermal parameters (*U* values) (2 pages); listings of calculated and observed structure factors (28 pages). Ordering information is given on any current masthead page.

---

(13) Angelici, R. J. *Acc. Chem. Res.* **1972**, *5*, 335.

(14) Cowie, A. G.; Johnson, B. F. G.; Lewis, J.; Nicholls, J. N.; Raithby, P. R.; Swanson, A. G. *J. Chem. Soc., Chem. Commun.* **1984**, 637.

(15) Braga, D.; Johnson, B. F. G.; Lewis, J.; McPartlin, M.; Nelson, W. J. H. *J. Chem. Soc., Chem. Commun.* **1982**, 966.

(16) Conner, J. A. In *Transition Metal Clusters*; Johnson, B. F. G., Ed.; Wiley: Chichester, U.K., 1980.